

# Passive seismic imaging in the presence of white noise sources

DEYAN DRAGANOV, KEES WAPENAAR, and JAN THORBECKE, Delft University, The Netherlands

Passive seismic imaging is based on the relation between the reflection and the transmission responses of the subsurface. Let one have the transmission responses measured at surface points A and B of a 3D inhomogeneous medium in the presence of white noise sources in the subsurface. When these transmission responses are cross-correlated, one obtains the reflection response of the same medium as if measured at point A in the presence of an impulsive source at point B. The quality of the simulated reflection response strongly depends on the whiteness and the distribution of the noise sources. Reflectors present below the sources cause the appearance of some ghost events. Random distribution of the noise sources will, however, weaken these ghost events.

Claerbout (1968) showed that by autocorrelating the transmission response of a 1D acoustic medium from noise sources in the subsurface, one can calculate the reflection response of the same medium. He named this method “acoustic daylight imaging.” Later, he conjectured that in order to simulate the reflection response of a 3D medium one needs to cross-correlate the transmission responses measured at different receivers. Wapenaar (2003) proved Claerbout’s conjecture for a 3D inhomogeneous medium. In the derivation it was assumed that there are no reflectors below the buried noise sources and that these sources are regularly distributed in the subsurface. In this paper, we investigate how restrictive this assumption is. In particular, we discuss some numerical modeling results with reflectors above as well as below the sources and with irregular distribution of the sources.

**Simulating reflection from transmission.** Let us have a 3D inhomogeneous domain  $D$ , which is lossless and source free (Figure 1), embedded between plan parallel boundaries  $\partial D_0$  and  $\partial D_m$ . Just above  $\partial D_0$  we have a free surface and below  $\partial D_m$  the half space is homogeneous. For this configuration, the reflection response can be calculated from the transmission response in the time domain using the relation (Wapenaar, 2003)

$$R(\mathbf{x}_B, \mathbf{x}_A, t) + R(\mathbf{x}_B, \mathbf{x}_A, -t) = \delta(\mathbf{x}_{H,B} - \mathbf{x}_{H,A}) \delta(t) - \int_{\partial D_m} T(\mathbf{x}_A, \mathbf{x}, -t) * T(\mathbf{x}_B, \mathbf{x}, t) dx \quad (1)$$

In this equation,  $R(\mathbf{x}_B, \mathbf{x}_A, t)$  denotes the reflection response including all free-surface and internal multiples of the domain  $D$  in the presence of a source at  $\mathbf{x}_A$  and a receiver at  $\mathbf{x}_B$  (Figure 1);  $T(\mathbf{x}_A, \mathbf{x}, t)$  denotes the transmission response including all free-surface and internal multiples of the domain  $D$  in the presence of a source at  $\mathbf{x}$  and a receiver at  $\mathbf{x}_A$  (Figure 2);  $*$  symbolizes temporal convolution;  $\mathbf{x}_{H,A}$  denotes the horizontal coordinates  $x_1$  and  $x_2$  of point A. The points with position vector  $\mathbf{x}_A$  and  $\mathbf{x}_B$  are situated at the free surface, just above the boundary  $\partial D_0$ . In the derivation of this relation, the evanescent wave modes have been neglected. Note that the left side of equation 1 contains the sum of the reflection response and its time-reversed version. Since the reflection response is causal, it is obtained by muting the noncausal part of the left-hand side of equation 1.

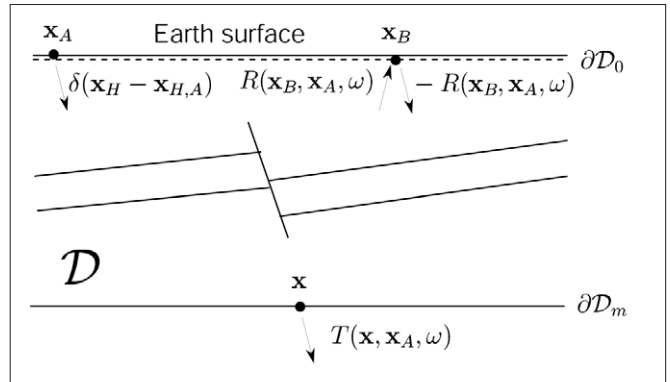


Figure 1. Domain  $D$  with its reflection response observed at the surface and with its transmission response observed in the subsurface.

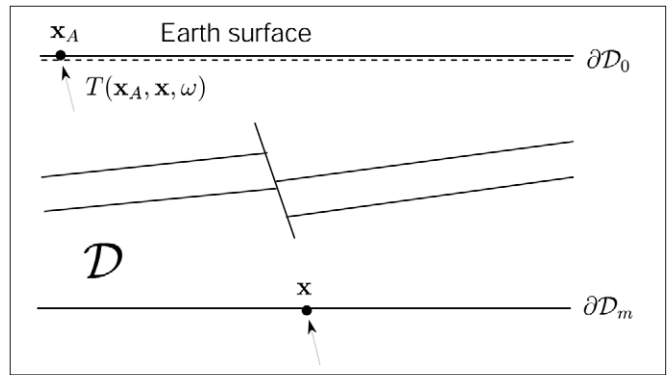


Figure 2. Domain  $D$  with its transmission response observed at the surface.

If in equation 1, the integral over the sources is discretized and the sources are assumed white and uncorrelated, then the relation can be rewritten as

$$R(\mathbf{x}_B, \mathbf{x}_A, t) + R(\mathbf{x}_B, \mathbf{x}_A, -t) = \delta(\mathbf{x}_{H,B} - \mathbf{x}_{H,A}) \delta(t) - T_{obs}(\mathbf{x}_A, -t) * T_{obs}(\mathbf{x}_B, t) \quad (2)$$

Here,

$$T_{obs}(\mathbf{x}_A, -t) = \sum_{\mathbf{x}_i \in \partial D_m} T(\mathbf{x}_A, \mathbf{x}_i, -t) * N_i(-t) \quad (3)$$

$$T_{obs}(\mathbf{x}_B, t) = \sum_{\mathbf{x}_j \in \partial D_m} T(\mathbf{x}_B, \mathbf{x}_j, t) * N_j(t) \quad (4)$$

represent the observed transmission responses of domain  $D$  recorded at the free surface in the presence of a number of discretely distributed uncorrelated white noise sources. In equations 2-4 the sources are along the boundary  $\partial D_m$ , but because the correlation process eliminates the extra traveltimes, it is plausible that the sources can be randomly distributed (Figure 3).

In the derivation of equations 1 and 2 it was assumed that the medium below the lower boundary  $\partial D_m$  of domain  $D$  is homogeneous, i.e. that there are no reflectors. What will happen when reflectors are present below the sources?

In the following, we discuss some 2D modeling results.

Editor’s note: This paper won the Best Student Poster Paper Award from the 2003 SEG Annual Meeting in Dallas.

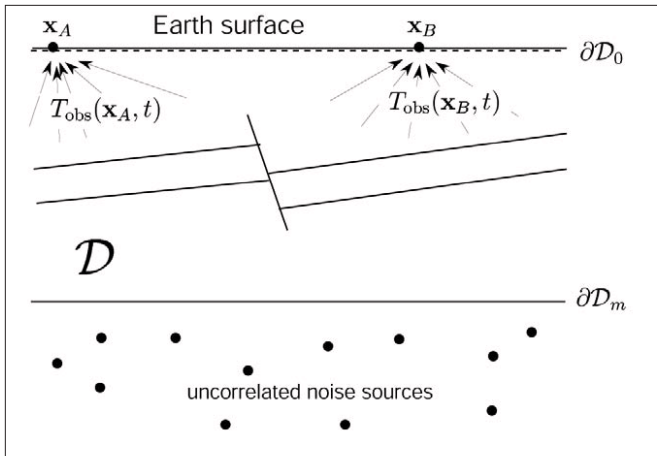


**Figure 3.** Transmission response recorded at positions  $x_A$  and  $x_B$  in the presence of white noise sources in the subsurface. According to equation (2), their cross-correlation yields the reflection response observed at  $x_B$  as if there were an impulsive point source at  $x_A$ .

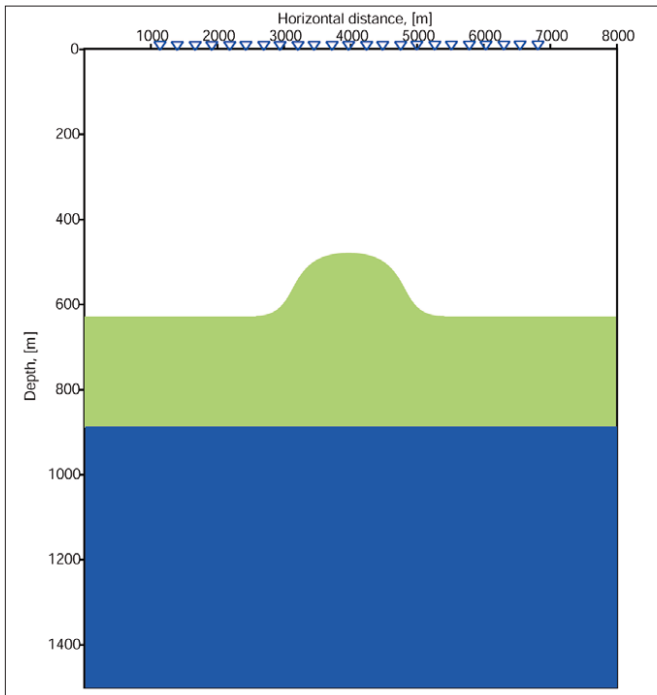


**Figure 4.** Anticline model used for the numerical simulations. The 23 blue triangles at the surface represent the 281 receivers starting at  $x_1=1200$  m and running until  $x_1=6800$  m.

As a model we take three layers with the first two layers separated by an anticline-shaped boundary. The acoustic velocity and the density for the layers are: top layer - 1500 m/s and 1000 kg/m<sup>3</sup>; middle layer - 2000 m/s and 3000 kg/m<sup>3</sup>; bottom layer - 2800 m/s and 4000 kg/m<sup>3</sup>. The receivers are regularly spaced at the surface every 20 m starting at position  $x_1=1200$  m and continuing until  $x_1=6800$  m. Figure 4 shows the anticline model and Figure 5 shows a zoomed in part of the model with three clusters of white noise sources at depth level  $x_3=750$  m. The first cluster is situated between horizontal distances 2500 and 3000 m, the second between 3750 and 4250 m, the third between 5000 and 5500 m. There are 101 sources within each cluster with a distance of 5 m between the sources. The transmission response  $T_{obs}$  of these 303 noise sources is shown in Figure 6 as a function of time and horizontal receiver position at the surface. The noise has been filtered with a tapered band-pass filter from 1 to 25 Hz. Using equation 2 we can calcu-

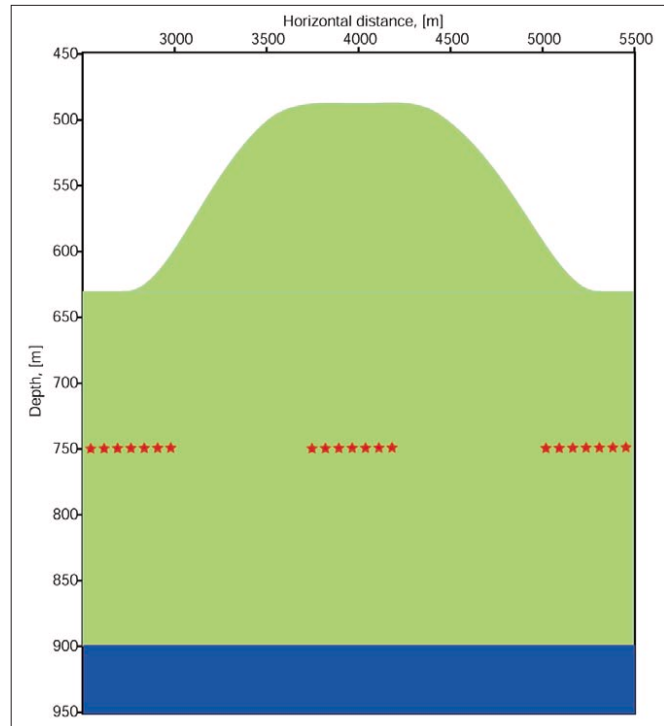


**Figure 5.** Zoomed in part of the model of Figure 4. The three clusters of seven red stars in this figure represent the three clusters of 101 white noise sources. In the clusters the sources are regularly distributed.

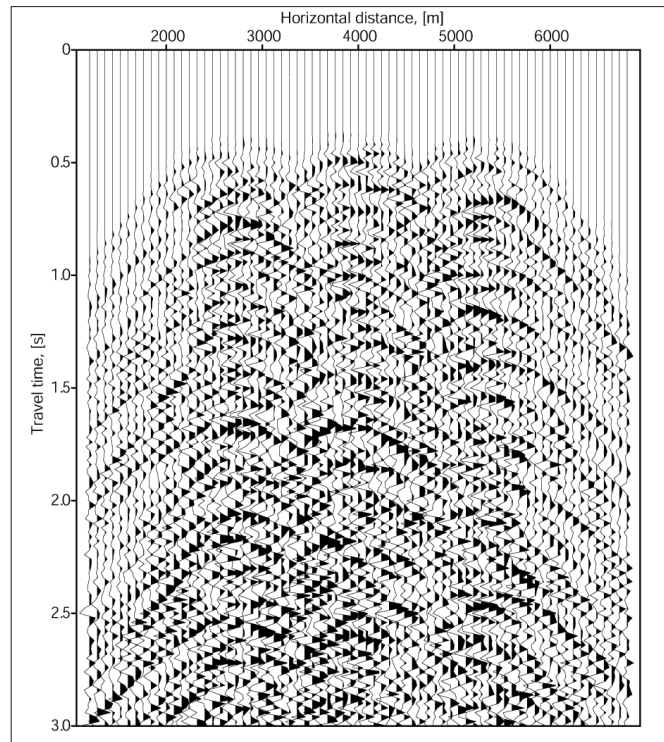


**Figure 6.** First 3 seconds from the 66-minute-long transmission panel,  $T_{obs}(t)$  from white noise sources in the subsurface.

late the reflection response  $R$  of the subsurface from the transmission response  $T_{obs}$ . To do this we extract one of the traces from the recorded transmission panel (in this case the trace at horizontal position  $x_1=4000$  m) and take it as the “master” trace  $T_{obs}(x_A, t)$  in equation 2. This master trace is then cross-correlated with all the traces in the transmission panel, each of which represents  $T_{obs}(x_B, t)$  in equation 2 (hence,  $x_B$  is now a variable). In the following examples 66-minute-long

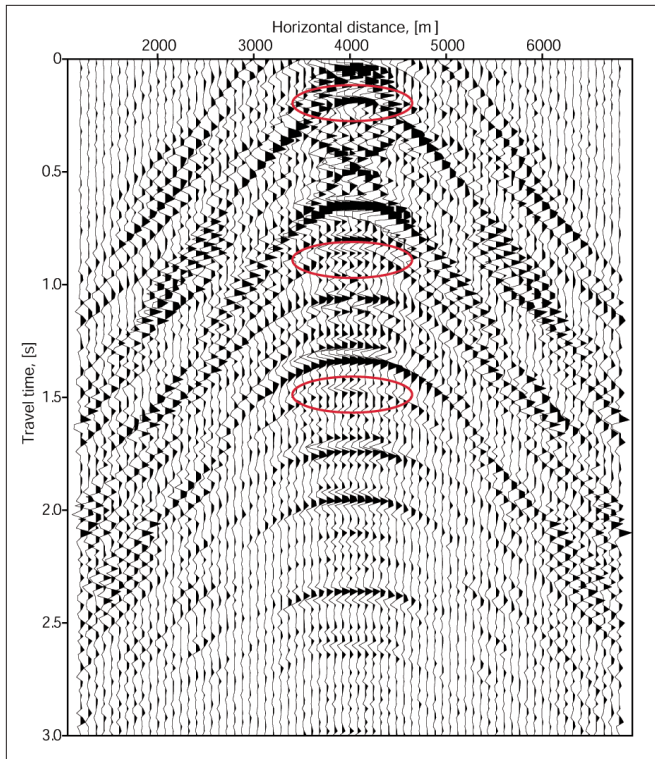


Figure 7. Simulated reflection response, obtained from the transmission response of the source clusters in of Figure 5.

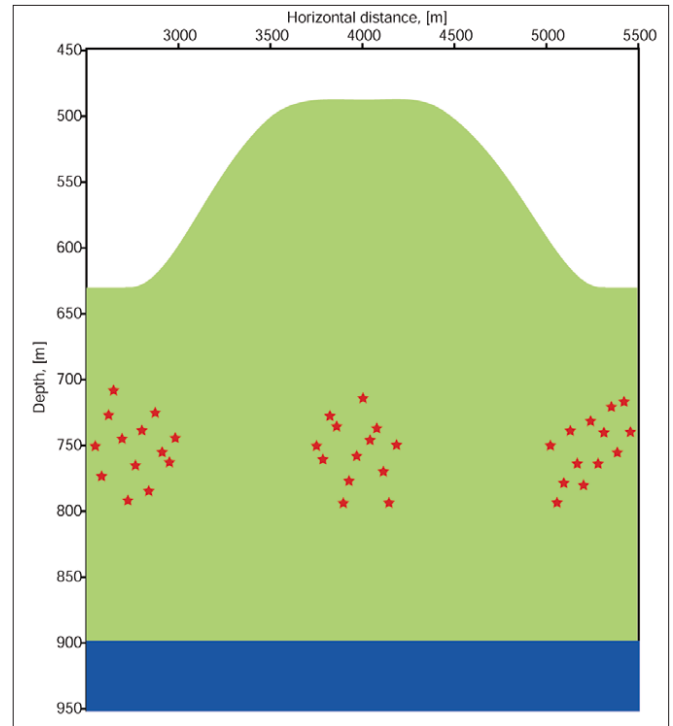


Figure 9. Zoomed in part of the model of Figure 4. The three clusters of 13 red stars in this figure represent the three clusters of 101 white noise sources. In the clusters the sources are randomly distributed in the vertical direction.

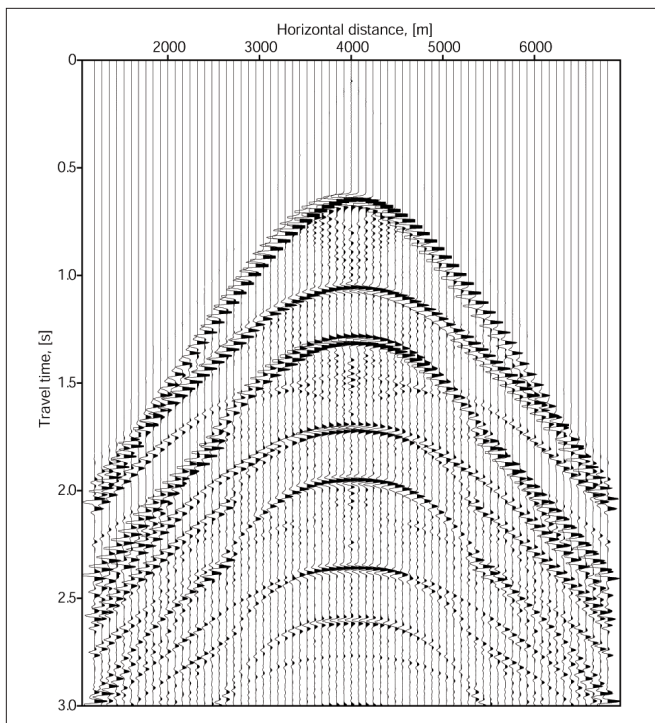


Figure 8. Directly modeled reflection response for the three layers model of Figure 4 with a seismic source (with a frequency band from 1 to 25 Hz) at the surface at position  $x_1=4000$  m.

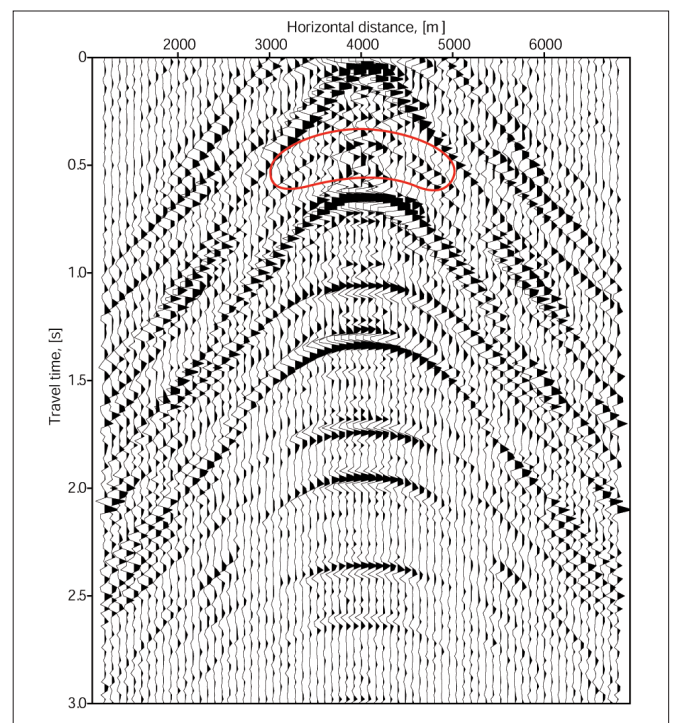
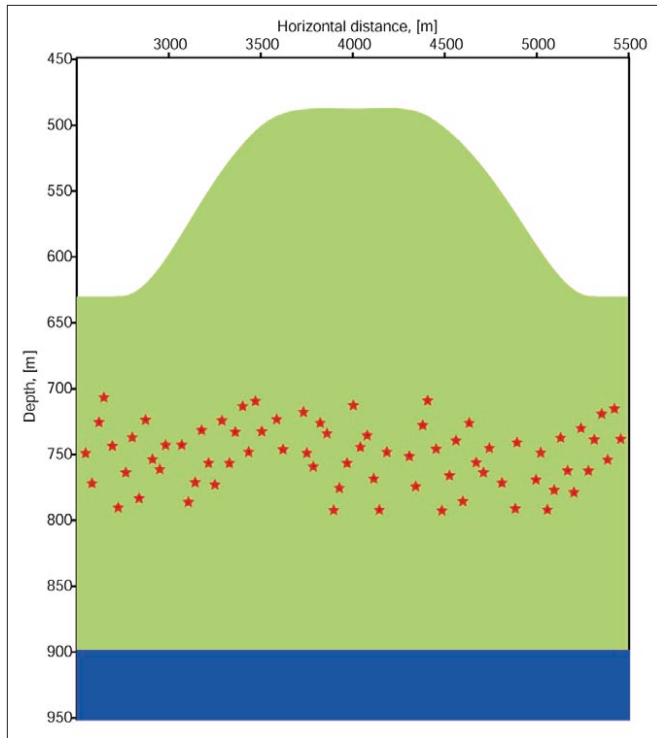


Figure 10. Simulated reflection response, obtained from the transmission response of the source clusters in Figure 9.

transmission records were used (Figure 6). After cross-correlating the transmission records and muting the noncausal part, we obtain the simulated reflection response as shown in Figure 7. This panel simulates a split-spread reflection survey with an impulsive source at the surface at  $x_1=4000$  m. The presence of the extra reflector at  $x_3=900$  m causes additional events to appear in the simulated reflection response.

Comparing the simulated reflection with the directly modeled reflection response (Figure 8), one can see that some events correctly represent real reflections, while others are ghost events (with apices in the red ellipses). The ghost event with apex at  $t=0.15$  s is a consequence of the correlation of the direct field from the subsurface sources with the wavefield that was first reflected at the interface



**Figure 11.** Zoomed-in part of the Figure 4 model. The 72 red stars represent one big group of 225 white noise sources (no big gaps between the sources) which are randomly distributed in the vertical direction.

below the sources and then recorded at the surface. The other two ellipses show the free-surface multiples of the first ghost event.

Figure 10 shows the simulated reflection response for the model of Figure 4, but now the sources in each cluster are randomly distributed in depth between levels 700 m and 800 m (Figure 9). Comparing this simulation with Figure 7, one sees that the ghost events we just discussed are strongly weakened. Comparing Figure 10 with the directly modeled reflection response (Figure 8) one notices another ghost event with apex at 0.45 s (inside the red area). This event is a result from the direct field in the transmission signals being internally reflected inside the second layer and then recorded at the surface. Note that the reflections that were correctly represented in Figure 7 are still correctly represented in the simulated reflection in Figure 10.

To see if the described ghost event with apex at 0.45 s is a result from the grouping of the noise sources in clusters, we simulated the reflection response for the model of Figure 11 where the noise sources are randomly distributed between depths 700 m and 800 m without big gaps between them. The result is shown in Figure 12. Comparing this result with the simulated reflection response in Figure 10, one notices that the ghost event with apex at 0.45 s is strongly weakened; i.e., the big gaps between the source clusters, in combination with the reflector below the sources, may indeed have caused this ghost event. Further, note that the simulated reflection response in Figure 12 exhibits better overall reconstruction in comparison with the simulated reflection response in Figure 10, where the middle part of the hyperbolic events is stronger (illuminated) than the

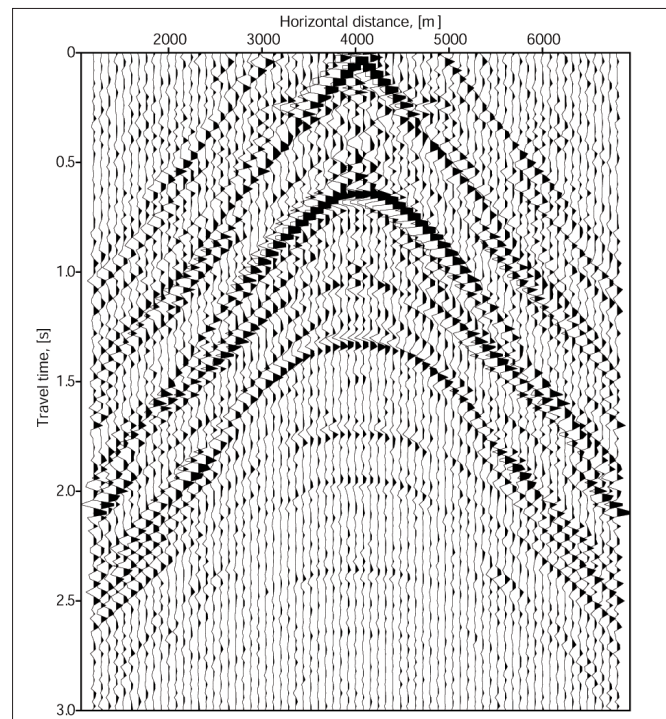


**Figure 12.** Simulated reflection response, obtained from the transmission response of the source distribution in Figure 11.

flanks because of the higher concentration of subsurface sources in that part of the model.

**Conclusions.** The numerical modeling results in this paper confirm relation 2 between the reflection and the transmission responses of a 3D inhomogeneous lossless medium in the presence of white noise sources in the subsurface. When reflectors are present below the buried sources, additional reflections, some of which are ghosts, appear in the simulated reflection response. The ghost events are strongly weakened, however, when the white noise sources have randomly distributed depths and when the reflectors above as well as below the subsurface sources are illuminated from all angles. Hence, we have shown that the underlying assumptions of equation 2 (regular distribution of sources; no reflectors below the sources) are not as restrictive as one would think intuitively.

**Suggested reading.** "Synthesis of a layered medium from its acoustic transmission response" by Claerbout (*GEOPHYSICS*, 1968). "Synthesis of an inhomogeneous medium from its acoustic transmission response" by Wapenaar (*GEOPHYSICS*, 2003). [TJE](#)

*Acknowledgments:* This modeling was done as part of a research project financed by the Dutch Science Foundation STW (grant DTN4915) and the Dutch Research Centre for Integrated Solid Earth Sciences - ISES.

*Corresponding author:* Deyan Draganov, D.S.Draganov@CiTG.TUdelft.nl